مجلة جمعية الليزر العراقية
Iraqi Laser Society Journal
I.L.S.J.
Issue-1 1st Year 2024

Formation and Possibility Detection of Initiated Electron Cloud in the Vicinity of Radioactive materials

Husham Abdul Maliek[1], Sawsan Khalaf Fandi[2] and Talib Z. Almosawi[3]

[1]Ministry of Science and Technology – Directorate of Nuclear Researches & Application

[2]Ministry of Science and Technology – Directorate of Materials Applications

[3]Kut College University

Hushamabid57@gmail.com

Abstract

This study presents a concept of forming high electron density cloud in the Vicinity of radioactive materials. The concept based on the reality that radioactive materials emit gamma rays, which ionize the surrounding air. The electrons generated due to ionization rapidly attach to oxygen molecules forming O_2^- ions. Density of O_2^- in the vicinity of radioactive material can be several orders of magnitude greater than background levels. Increased population of O_2^- extends several meters around the radioactive material. Electrons are easily photo-detached from O_2^- ions by a radiation of THz pulse signal. In the presence of THz pulse radiation, the photo-detached electrons initiate avalanche ionization which results in a rapid increase in electron density. As the electron density increases a frequency modulation on a probe beam will be induced, this becomes a direct spectral signature for the presence of radioactive material. Three radioactive sources are introduced in this study, ^{60}Co, ^{137}Cs and ^{22}Na. These three radioactive sources of different amount 1.0 mg and 20.0 mg. The calculations are done up to three meters away from the sources. THz radiation could be high intensity laser source.

Keywords: Radioactive, Gamma ray, Ionization, Electron Density, Photo-Detached.

تشكل غيمة الالكترونات الناشئة في محيط المواد المشعة و امكانية كشفها

هشام عبد الملك[1]، سوسن خلف فندي[2]، طالب زيدان تبان[3]

[1]وزارة العلوم و التكنولوجيا – مديرية البحوث و التطبيقات النووية

[2]وزارة العلوم و التكنولوجيا – دائرة بحوث المواد

[3]قسم الفيزياء ، كلية العلوم ، الجامعة المستنصرية

الخلاصة

تقدم دراسة هذا البحث فكرة لتشكل غيمة البلازما في محيط المواد المشعة. تستند الفكرة على حقيقة ان المواد المشعة تبعث اشعة گاما و التي لها القابلية على تأيين الهواء المحيط بها. ترتبط الالكترونات المؤينة سريعا بجزيئات الاوكسجين مشكلة بذلك آيون الاوكسجين السالب. تكون كثافة آيونات الاوكسجين السالبة حول المادة المشعة اكبر بعدة مئات من المرات مقارنة بمستويات الخلفية الطبيعية للهواء. يمتد تعداد آيونات الاوكسجين السالبة عدة امتار حول المادة المشعة. يمكن ازاحة الالكترونات بسهولة من آيونات الاوكسجين بواسطة فوتونات اشعة ذات شدة عالية و تردد THz. تنشئ الالكترونات المزاحة فوتونيا بفعل اشعة THz تأينا انهياريا مما يترتب عليه زيادة كثافة الالكترونات. تحث زيادة كثافة البلازما المتولدة تضمينا ترددیا على متحسس حزمة الاشعاع النبضي و الذي يشكل بصمة طيفية مباشرة تؤكد وجود مادة مشعة. اجريت الدراسة باستخدام ثلاثة مصادر مشعة هي ^{60}Co، ^{137}Cs و ^{22}Na . استخدمت كميات مختلفة من هذه المواد بقدر 1 و 20 ملغم. اجريت الحسابات لمسافة لاتتجاوز الامتار الثلاثة عن المصادر المشعة .يمكن ان يكون مصدر اشعاع THz مصدرا ليزريا ذو شدة عالية.

Introduction

Generally, gamma rays emitted by radioactive materials, which ionize the surrounding air producing free electrons which are rapidly attach to oxygen molecules forming O_2^- ions. The density of negative ions is far greater than the free electron density [1, 2]. This is true even for ambient levels of radioactive material. A recently proposed radioactivity detection concept based on a high power THz pulse inducing avalanche breakdown and spark formation in the vicinity of the radioactive material. [3–6] in that concept, a THz pulse focused to a volume $V_{f\ ocal}$ near the radioactive material. In the absence of the radioactive material, the electron density N_e is sufficiently small so that $N_e\ V_{f\ ocal} << 1$. In this case, the probability of n electron appearing in the focal volume during the THz pulse is negligible, and the breakdown probability is very low. In the presence of radioactivity, however, $N_e V_{f\,ocal} \geq 1$, will lead to avalanche ionization in the volume $V_{f\,ocal}$ occurs provided the THz pulse intensity is above a threshold level and the pulse length is sufficiently long. Breakdown and spark formation requires that the collisional ionization rate exceed the attachment rate. A THz-based radioactivity detection concept may have unique advantages depending on the stand-off distance and atmospheric conditions [7-10].

Radiation enhancement factor

A gamma ray propagating through matter can interact through several processes, including Rayleigh scattering, photoelectric and Compton effects, pair production, etc [11] .In air, photoelectric absorption dominates at low photon energies (< 25 keV) while at high energies (~ 25 keV–3MeV) Compton processes dominate. As the gamma ray propagates in air, it loses energy in a cascading process and its mean free path L_γ decreases. Gamma rays having energies of 1MeV, 50 keV, 25 keV, or 10 keV, have mean free paths in air of $L_\gamma \approx 130$ m, 38 m, 19 m, or 1.9 m, respectively. Note that values for the range indicated here apply to the case where a gamma ray with the given energy is completely absorbed in a single interaction (collision). The actual mean free path for a given initial energy is somewhat less than that for a single interaction.

The ionization rate due to background (ambient) radioactivity is $(dN_e/dt)_{amb} = Q_{rad}$. At or near ground level, the background ionization rate is typically in the range $Q_{rad} \sim 10–30$ pairs/cm^3.s. The gamma rays emitted by radioactive material ionize the surrounding air. In the presence of radioactive material, the ionization rate (due to only radiation) can be greatly enhanced by a factor $\alpha_{rad} >> 1$ and $(dN_e/dt)_{amb} = \alpha_{rad}\, Q_{rad}$. .

The enhancement factor α_{rad} can be estimated as follows, For a radioactive material of mass M_{rad} , the number of disintegrations per second is $\gamma_{rad} = M_{rad}\, A_{rad}$, where A_{rad} is the specific activity associated with the material.

In air, for high energy gammas high energy electrons generated, via Compton and photoelectric processes, which undergo a cascading process to sufficiently low energy to attach to O^2 molecules forming O_2^- ions. In the cascading process, the electrons lose an amount of energy $\Delta E \approx 35$ eV per collision in air, which results in both ionization and electronic excitation (~ equal amounts of energy lost to each process) [12]. A high energy electron with energy E_e therefore generates ~ $E_e / \Delta E$ low energy electrons. In the case of Compton absorption, the maximum electron energy is:

$E_e = (2\alpha_\gamma / (1+ 2\alpha_\gamma)) E_{\gamma \cdot max}$,

where $\alpha_\gamma = E_{\gamma \cdot max} / mc^2$.For example, a 1MeV gamma ray in air generates Compton electrons having a maximum energy of E_e = 0.8MeV and average energy of ‹Ee› = 0.44MeV. It should be noted that the range of high energy electrons is much less than the range of the high energy gammas.

The steady state density of emitted gamma rays for a small spherical source of radioactivity is

$$N_\gamma = \frac{\nu_{rad} K_\gamma}{4\pi C R^2} exp(-R/L_\gamma) \ldots\ldots (1)$$

where R stands for radioactive material distance, L_γ is the effective range (mean free path) of the gamma rays in air, which is a function of the gamma ray energy, E_γ, and K_γ is the number of gammas emitted per disintegration. The rate change of electron density is given by

$$\frac{\partial Ne}{\partial t} \approx (\alpha_{rad} + 1) Q_{rad} + airchemistryandionizationterms\ldots$$

Where

$$\alpha_{rad} \approx C(\sigma_{\gamma-e}) N_{air} N_\gamma \frac{\langle E_e \rangle}{\Delta E} \frac{1}{Q_{rad}}$$

$$\approx \frac{\gamma_{rad} K_\gamma}{4\pi \langle L_{\gamma-e} \rangle} \frac{\langle E_e \rangle}{\Delta E} \frac{1}{Q_{rad}} \frac{exp(-R/L_\gamma)}{R^2} \ldots\ldots (3)$$

is the radiation enhancement factor. An equivalent result defining the detectable mass of the radioactivity material as a function of the various parameters was obtained in Ref.[6].In the absence of radioactive material, α_{rad} = 0. In Eq. (3) $\langle \sigma_{\gamma\text{-}e} \rangle$

$= \langle\sigma_{\gamma\text{-}e}\rangle_{CA} + \langle\sigma_{\gamma\text{-}e}\rangle_{PE}$ is the effective average cross section for electron generation by gammas, i.e., Compton absorption and photoelectric processes, $\langle L_{\gamma\text{-}e}\rangle = (\langle\sigma_{\gamma\text{-}e}\rangle)\ N_{air})^{-1}$ is the average mean free path for electron generation by gammas and $N_{air} = 2.7 * 10^{19}\ cm^{-3}$ is the air density (Loschmidt's number) at STP. The cross section $\sigma_{\gamma\text{-}e}$ (E) is a function of the gamma ray energy and the average cross-section is given by $\langle\sigma_{\gamma\text{-}e}\rangle = \int dE\ f(E)\ \sigma_{\gamma\text{-}e}(E)$, where f (E) is the gamma ray energy distribution function.

Over the range of energies ~ 0.05-1 MeV, Compton absorption dominates and $\langle\sigma_{\gamma\text{-}e}\rangle_{CA} \sim 1.4 * 10^{-24}\ cm^2$, while for energies below ~ 0.05MeV the photoelectric effect dominates with $\langle\sigma_{\gamma\text{-}e}\rangle_{PE}$ growing from $\sim 1.4 * 10^{-24}\ cm^2$ at 0.05MeV to $\sim 2 * 10^{-22}\ cm^2$ at 0.01MeV.

Electron and ion density evolution

To determine the frequency modulation on a probe pulse, it is necessary to follow the time evolution of the electron and negative ion density, which are sensitive functions of electron heating by the laser radiation [13]. The source terms for the electrons include radioactivity, detachment, photo-detachment and photo-ionization, while the loss terms include various attachment and recombination processes including aerosols.

The expressions for the rate of change of electron density N_e and negative ion density $N\_$ are [14–17]

$$\partial N_e / \partial t = (1 + \alpha_{rad})\ Q_{rad} + S_e - L_e, \quad (4a)$$

$$\partial N\_ / \partial t = S\_ - L\_, \quad (4b)$$

where S_e represents the various electron source terms, L_e is the electron loss terms, $S\_$ represents the ion source, $L\_$ is the ion loss terms. The effect of radioactivity is represented by the first term on the right hand side of the electron rate equation (4a). As the free electron density is generally much less than the ion density, $N_e << N\_$ densities of electron and negative ion at the steady state are found to be given by:

$$N_e \approx (\beta_n N_n / \eta)\ (\surd\ (1 + \alpha_{rad})\ Q_{rad} / \beta_+) + (1 + \alpha_{rad})\ Q_{rad} / \eta$$

$\approx \beta_n N_n / \eta) (\surd (1 + \alpha_{rad}) Q_{rad} / \beta_+)$, and

$N_- \approx \surd (1 + \alpha_{rad}) Q_{rad} / \beta_+$ [4]

where N_n is the neutral air density ($N_n \sim N_{air}$ for low levels of ionization), $\beta_+ \approx 2 * 10^{-6}$ cm^3/s is the recombination rate, $\eta \approx 10^8$ s^{-1} is the attachment rate, and $\beta_n \approx (5–10) *10^{-19}$ cm^3/s is the negative ion detachment rate due to collisions with neutrals.

Methodology of the study

The growing population of O_2^- extends several meters around the radioactive material. Electrons are easily photo-detached from O_2^- ions by a radiation of THz pulse signal. The photo-detached electrons, in the presence of THz pulse radiation, initiate avalanche ionization which results in a rapid increase in electron density. The increasing in electron density induces a frequency modulation on a probe beam, which becomes a direct spectral signature for the presence of radioactive material.

Frequency of plasma, ω_p, initiated by electron density, N_e, is given by [18]:

$\omega_p (z, t) = (4\pi q^2 N_e) (z, t) /m)^{1/2}$ ……….(5)

The photo-detachment rate is: $\nu_{opt} = \sigma_{opt} cN_{ph} = \sigma_{opt} I_o / \hbar\omega$, where $cN_{ph} = I_o/\hbar\omega$ .... (6)

the incident photon flux, I_o the radiation intensity and σ_{opt} the photo-detachment cross section.

The experimental value for the single-photon photo-detachment cross section of O_2^- is σ_{opt} (λ = 1 μm) ≈ 4.5 * 10^{-19} cm^2 and σ_{opt} (λ = 0.8 μm) ≈ 7.5 * 10^{-19} cm^2 [16]. The single-photon photo-detachment rate for O_2^- is therefore: ν_{opt} [sec^{-1}] = I_o [W/ cm^2] = 2.3, λ = 1 μm or 3, λ = 0.8 μm.

For the parameters considered here, multiphoton ionization of air can be neglected since the ionization potential for clean air (O_2) is ~ 12 eV and requires ~ 8–10 photons.

A probe beam propagating through a vicinity of radioactive material which the electron density is changing with time will undergo a frequency change. The electron density in the vicinity of the radioactive source and under the influence of the THz radiation varies in space and in time.

The frequency modulation on the probe beam is given by $\omega_{probe}(z, t) = \omega_o + \Delta \omega (z, t)$, where ω_o is the incident probe frequency and $\Delta \omega$ is given as [19]:

$\Delta \omega (z, t) = \omega_{po}^2 / (2 \omega_o) \exp (vion\ t) (1 - \exp(- v_{ion} z/c))$ …….. (7)

where v_{ion} is the effective ionization rate.

Result and Discussion

In this study three different radioactive materials (sources) are applied, ^{60}Co, ^{137}Cs and ^{22}Na. The amounts of these three radioactive materials are 1.0 mg and 20 mg. Ranges of testing the radiation in vicinity of these materials are ranging from 0.5 m to 3.0 m.

Some important information about the two radioactive materials is in table (1)

Table (1) important information about the two radioactive materials

Radioactive material	Specific Activity (Ci / g)	Number of Energy peaks	Peak Energy (Mev)
^{60}Co	1143.5	Two	E_1=1.173 E_2=1.332
^{137}Cs	87.77	One	E_1= 0.666
^{22}Na	6316.8	Two	E_1= 0.511

In Figures below, density of emitted gamma rays, N_γ (cm^{-3}), electron density for air due to emitted gamma rays, N_e (cm^{-3}), negative ion density of photo detachment for air due to emitted gamma rays, N_- (cm^{-3}), and radiation enhancement factor α_{rad} is plotted as a function of the distance from the radioactive source, R.

Below are plots for density of emitted gamma rays, N_γ (cm^{-3}), versus range for different amounts of ^{60}**Co**, ^{137}**Cs** and ^{22}**Na** seeing Fig. [1].

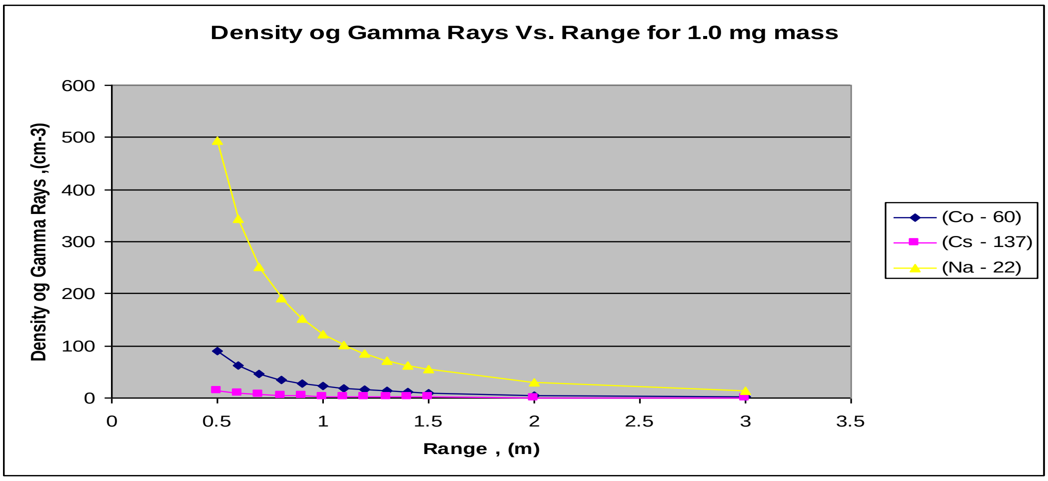

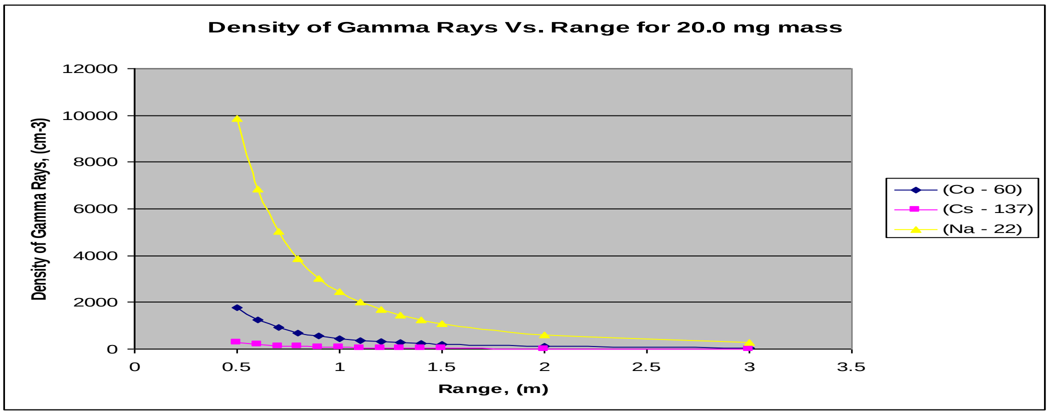

Fig. [1]. Show plots for density of emitted gamma rays, N_γ (cm^{-3}), versus range for different amounts of the three radioactive sources.

Below are plot for electron density for air due to emitted gamma rays, N_e (cm^{-3}), versus range for different amounts ^{60}**Co**, ^{137}**Cs** and ^{22}**Na,** seeing Fig. [2].

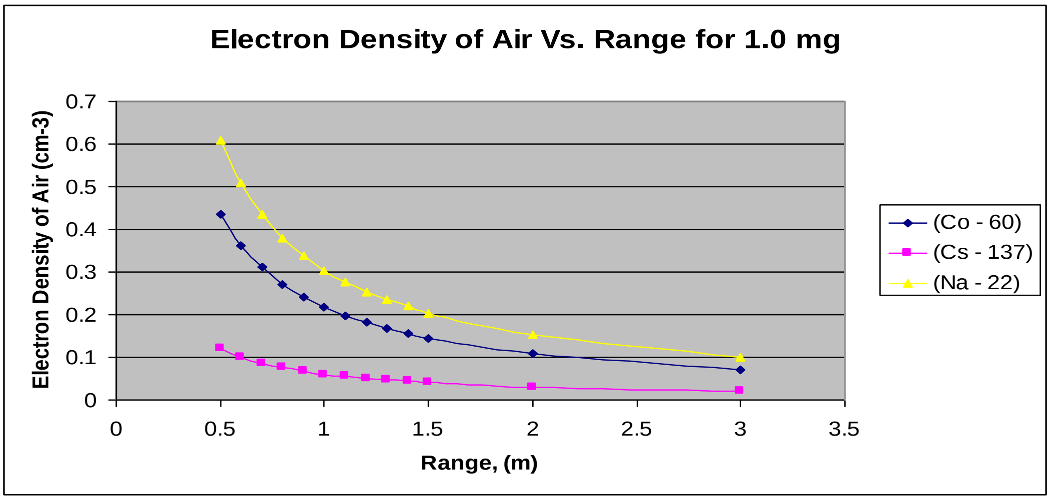

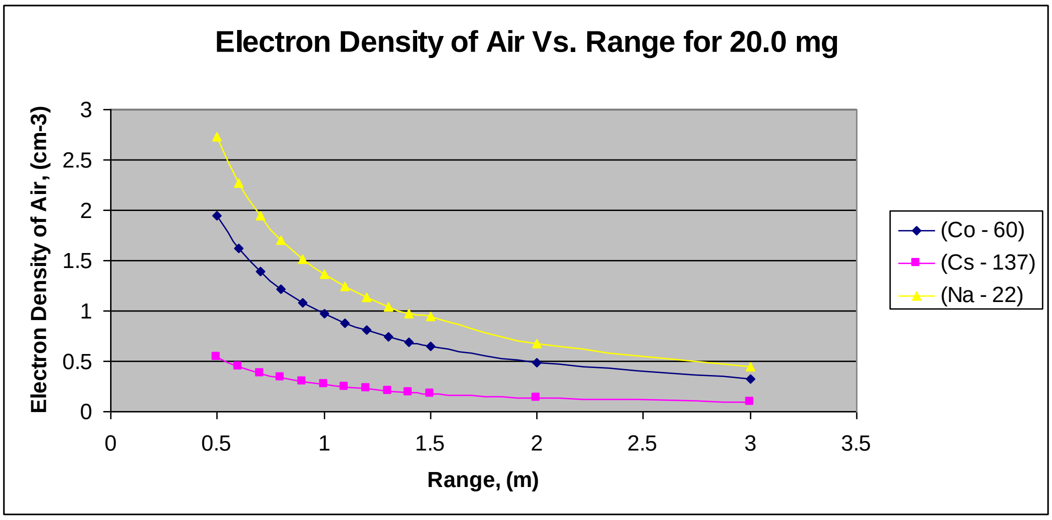

3

Fig. [2]. show plot for electron density for air due to emitted gamma rays, N_e (cm^{-3}), versus range for different amounts of the three radioactive sources.

Below are plot for negative ion density of photo detachment for air due to emitted gamma rays, N_- (cm^{-3}), versus range for different amounts of ^{60}**Co**, ^{137}Cs and ^{22}**Na**, seeing Fig. [3].

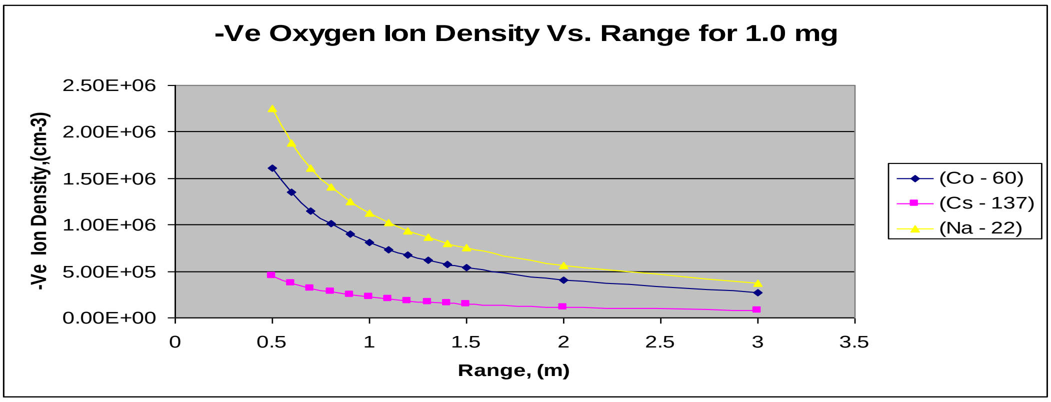

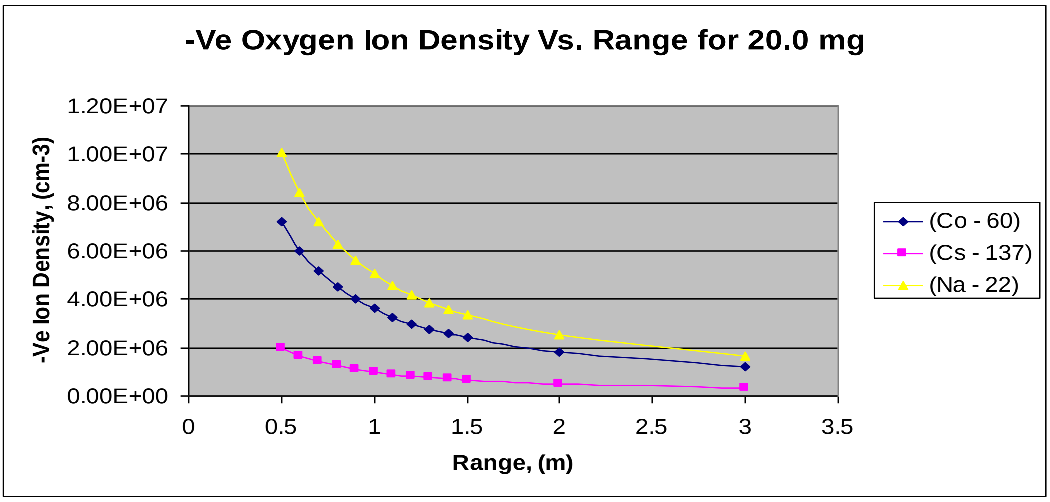

Fig. [3]. show plots for negative ion density of photo detachment for air due to emitted gamma rays, N_- (cm^{-3}), versus range for different amounts of the three radioactive sources.

Below are plot for Radiation Enhancement factor, ionization rate due to radiation, α_{rad} versus range for different amounts of ^{60}**Co**, ^{137}**Cs** and ^{22}**Na,**seeing Fig. [4].

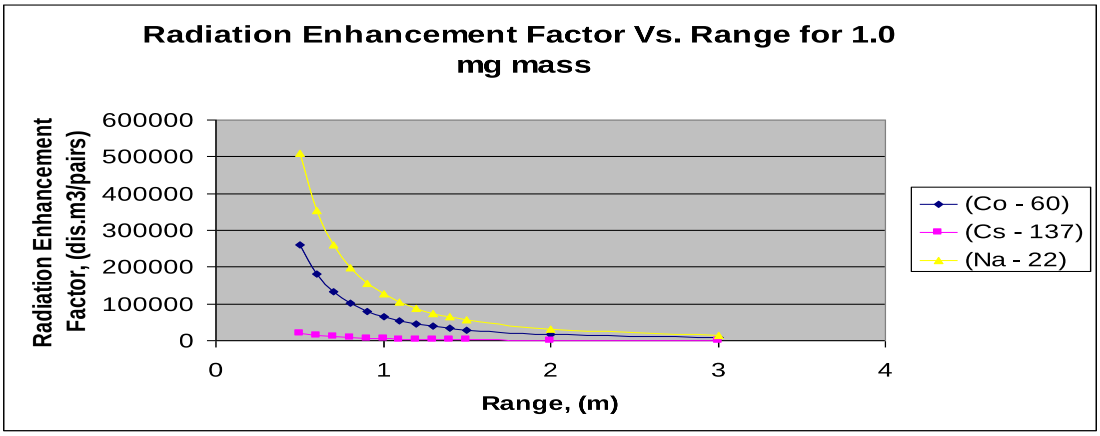

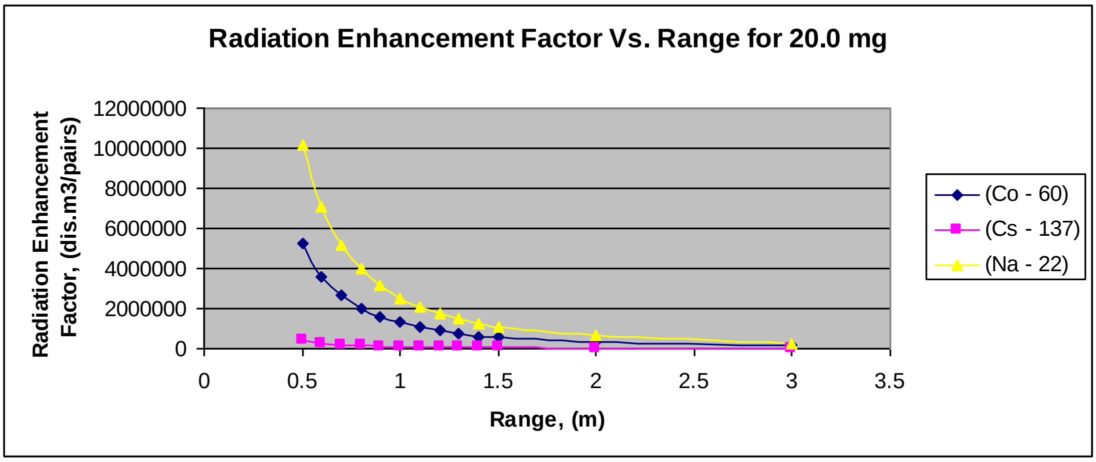

Fig. [4]. show plots for Radiation Enhancement factor, ionization rate, due to radiation, α_{rad} versus range for different amounts of the three radioactive sources.

The negative ion, O_2^-, undergoes single-photon photo-detachment with radiation of wavelength λ = 1 μm (1.24 eV) or λ = 0.8 μm(1.55 eV) because the electron affinity of O_2^- is low enough ,0.46 eV, for this process.

So, by applying high intensity THz beam of the λ = 1.0 μm or, λ = 0.8 μm in the vicinity of radioactive material an electromagnetic signature is registered due to the rise of the electron density at the end of the ionizing laser pulse which approaches the value of $N_e=10^{14}$ cm^{-3}.

Conclusion

This study showed the possibility of detecting dense electron cloud initiated by a radioactive material even at small quantities. Forming O_2^- could be ionized by a high intensity THz radiation making an avalanche breakdown to photo detach the electrons from O_2^- forming a cloud of electron density much more several orders of magnitude than background levels. Also, it showed different quantities and different specific activity give different densities of emitted gamma rays, electron densities, negative ion densities of photo detachment and radiation enhancement factors, all are versus range from the radioactive material. Applying a high intensity THz beam of the λ = 1 μm or, λ = 0.8 μm in the vicinity of radioactive material an electromagnetic signature is registered due to the rise of the electron density. This signature is a solid proof of existence of a radioactive material.

References

[1] W. A. Hoppel,"The Earth’s Electrical Environment" (The National Academies Press, 1986), p. 149.

[2] A. J. Peurrung, Nucl. Instrum. Methods Phys. Res., Sect. A 481, 731 (2002)

[3] V. L. Granatstein and G. S. Nusinovich, J. Appl. Phys. 108, 063304 (2010)

[4] G. S. Nusinovich, P. Sprangle, C. R. Talamas, and V. L. Granatstein, J. Appl. Phys. 109, 083303 (2011).

[5] G. S. Nusinovich, R. Pu, T. M. Antonsen, O. V. Sinitsyn, J. Rodgers, A. Mohamed, J. Silverman, M. Al-Sheikhly, Y. S. Dimant, G. M. Milikh, M.Yu, Glyavin, A. G. Luchinin, E. A. Kopelovich, and V. L. Granatstein, J. Infrared Millim. THz Waves 32, 380 (2011).

[6] Y. S. Dimant, G. S. Nusinovich, P. Sprangle, J. Pe~nano, C. A. Romero-Talamas, and V. L. Granatstein, J. Appl. Phys. 112, 083303 (2012).

[7] P. Sprangle, J. R. Pe~nano, and B. Hafizi, Phys. Rev. E 66, 046418 (2002).

[8] A. Ting, I. Alexeev, D. Gordon, E. Briscoe, J. Penano, R. Fischer, R. Hubbard, P. Sprangle, and G. Rubel, Appl. Opt. 44, 5315 (2005).

[9] S. Varma, Y.-H. Chen, and H. M. Milchberg, Phys. Rev. Lett. 101, 205001 (2008).

[10] S. Eisenmann, J. Pe~nano, P. Sprangle, and A. Zigler, Phys. Rev. Lett. 100, 155003 (2008)

[11] American Institute of Physics Handbook, 3rd ed., edited by D. E. Gray (McGraw-Hill, New York, 1972), pp. 8–203.

[12] M. H. Rees, "Physics and Chemistry of the Upper Atmosphere" (Cambridge University Press, Cambridge, UK, 1989), p. 40

[13] M. Capitelli, C. M. Ferreira, B. F. Gordiets, and A. I. Osipov, Plasma Kinetics in Atmospheric Gases (Springer-Verlag, NY, 2010).

[14] R. F. Fernsler, A. W. Ali, J. R. Greig, "The NRL CHMAIR Code: A Disturbed Sea Level Air Chemistry

Code", NRL Memorandum Report No. 4110, 1979.

[15] A. W. Ali, "Electron Energy Loss Rates in Air", NRL Memorandum Report No. 5400, 1984.

[16] L. G. Christophorou, "Atomic and Molecular Radiation Physics" (Wiley-Interscience, London, UK, 1971), p. 530.

[17] P. Sprangle, J. Pe~nano, B. Hafizi, D. Gordon, and M. Scully, Appl. Phys. Lett. 98, 211102 (2011).

[18] Y. B. Zel'dovich and Y. P. Raizer, "Physics of Shock Waves and High-Temperature Hydrodynamic Phenomena" (Dover, Mineola, NY, 2002).

[19] R. Schunk and A. Nagy, Ionospheres (Cambridge University Press,

Cambridge, UK, 2009).